

Study of copper substitutions in $\text{Ag}(\text{Nb}_x\text{Ta}_{1-x})\text{O}_3$ solid solutions

Sonia Duguey^{a,*}, Richard Lebourgeois^b, Claude Grattepain^b,
Jean-Marc Heintz^c, Jean-Pierre Ganne^b

^a Temex Ceramics, Pl Bersol, Voie Romaine, 33600 Pessac, France

^b THALES R&T, RD 128, 91767 Palaiseau, France

^c ICMCB-Institut de Chimie de la Matière Condensée de Bordeaux, 87 Av. Dr Schweitzer, 33608 Pessac, France

Available online 30 June 2006

Abstract

This study deals with the effect of copper in $\text{AgNb}_{1-x}\text{Ta}_x\text{O}_3$ solid solutions (ANT). Firstly, CuO was added after calcination and used as a sintering aid. Secondly, copper oxide was introduced as a raw material by substituting a part of Ag_2O , Nb_2O_5 or Ta_2O_5 . Compositions were made using conventional ceramics route. The powder processing and the firing conditions were optimized.

For all formulations, silver precipitates were observed inside the ceramics. The lowest dielectric losses were obtained for Ag_2O deficiency samples sintered at 915 °C in oxygen atmosphere. With a permittivity of 415 and a $Q \times f = 610$ GHz, these compositions exhibited better dielectric properties than CuO added samples. These characteristics are very promising for filtering applications in the radio-frequency range.

© 2006 Elsevier Ltd. All rights reserved.

Keywords: Spectroscopy; Dielectric properties; Perovskites; Capacitors; ANT ($\text{AgNb}_{1-x}\text{Ta}_x\text{O}_3$)

1. Introduction

With the rapid progress of wireless communication systems, the development of LTCC materials (low-temperature cofired ceramics) in the passive-component and packaging industries has found renewed interest. LTCC technology requires materials with low loss for high frequency applications and a high dielectric constant for integration of embedded capacitor components and resonators.

Moreover, dielectrics must be sintered at low temperature and be compatible with low-loss conductors, such a silver.

Previous studies indicated that ANT perovskites have an interesting potential as a material for wireless-telecommunication technology due to low dielectric losses combined with a very high permittivity.^{1,2} To decrease the sintering temperature, Kim et al. proposed some sintering aids.³ They have noticed that CuO addition after calcination allowed both to reduce the sintering temperature of about 300 °C (making possible co-firing with silver) and to keep good dielectric properties.

The objective of this work was to synthesize low sintering temperature dielectrics with a high dielectric constant and low losses.

Sintering behaviour of compositions where copper oxide was used as raw material (noted copper substituted ANT) in comparison with compositions where copper oxide was added after calcination (noted copper oxide added ANT) was investigated. Niobium oxides with fine and large grain size were used, respectively, to reduce the sintering temperature.

Microscopy analysis was conducted to examine the CuO location in the polycrystalline samples. Permittivity and dielectric losses were measured from 40 Hz to 2 GHz for all samples.

2. Experimental procedure

Copper substituted ANT were synthesized using the solid-state chemical reaction method. Ag_2O (Alfa Aesar, 0.35 m²/g), Ta_2O_5 (Alfa Aesar, 2.8 m²/g), Nb_2O_5 (Alfa Aesar, 0.3 m²/g or HJD, 8.35 m²/g) and CuO (Merck, 4.9 m²/g) were chosen as starting raw materials. We substituted CuO for Ag_2O , Nb_2O_5 , Ta_2O_5 (Table 1). A previous study has concluded that 1 wt.% CuO addition gave full densification. So, the corresponding copper mole content was chosen for the formulations preparations. The powder mixtures were weighed and then mixed, using attrition-milling with cerium–zirconia balls in H_2O for 1 h. According to the Nb_2O_5 grain size, the mixed powders were calcined at 740 °C (Nb_2O_5 HJD) or 900 °C (Nb_2O_5 Alfa) for 2 h in air and then milled for 30 min. The ground powders were granu-

* Corresponding author. Tel.: +33 169415901; fax: +33 169415738.
E-mail address: sonia.duguey@thalesgroup.com (S. Duguey).

Table 1

Targeted compositions for copper substitutions in $\text{Ag}(\text{Nb}_x\text{Ta}_{1-x})\text{O}_3$ solid solutions

Site	Substituted elements	Raw material mixture	Targeted compositions
B	Nb	$0.5\text{Ag}_2\text{O} + 0.232\text{Nb}_2\text{O}_5 + 0.25\text{Ta}_2\text{O}_5$	$\text{Ag}(\text{Nb}_{0.463}\text{Cu}_{0.037})\text{Ta}_{0.5}\text{O}_{3-\delta}$
	Ta	$0.5\text{Ag}_2\text{O} + 0.25\text{Nb}_2\text{O}_5 + 0.232\text{Ta}_2\text{O}_5 + 0.037\text{CuO}$	$\text{AgNb}_{0.5}(\text{Ta}_{0.463}\text{Cu}_{0.037})\text{O}_{3-\delta}$
A	Ag	$0.482\text{Ag}_2\text{O} + 0.25\text{Nb}_2\text{O}_5 + 0.25\text{Ta}_2\text{O}_5 + 0.037\text{CuO}$	$(\text{Ag}_{0.963}\text{Cu}_{0.037})\text{Nb}_{0.5}\text{Ta}_{0.5}\text{O}_{3-\delta}$

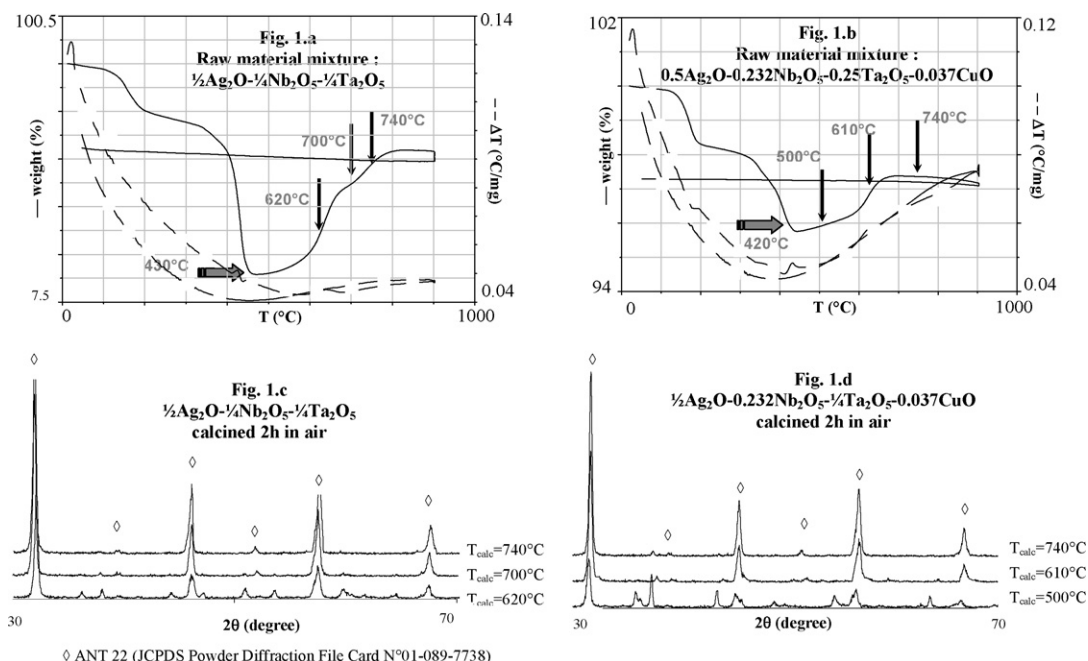


Fig. 1. Observation of the phase formation using TGA/TDA and XRD: (a) TGA/DTA on $(1/2)\text{Ag}_2\text{O}-(1/4)\text{Nb}_2\text{O}_5-(1/4)\text{Ta}_2\text{O}_5$ —firing rate 20°C/h ; (b) TGA/DTA on $0.5\text{Ag}_2\text{O}-0.232\text{Nb}_2\text{O}_5-0.25\text{Ta}_2\text{O}_5-0.037\text{CuO}$ —firing rate 20°C/h ; (c) XRD after calcination 2 h in air for $(1/2)\text{Ag}_2\text{O}-(1/4)\text{Nb}_2\text{O}_5-(1/4)\text{Ta}_2\text{O}_5$; (d) XRD after calcination 2 h in air for $0.5\text{Ag}_2\text{O}-0.232\text{Nb}_2\text{O}_5-0.25\text{Ta}_2\text{O}_5-0.037\text{CuO}$.

lated by mixing them in poly(vinyl) alcohol (PVA) solution, and then the granules were pressed into disks with 9 mm in diameter and 8.5 or 1 mm thick, for resonators or capacitors, respectively. The disks were sintered at different temperature and atmosphere.

Copper oxide added ANT was synthesized using the same route, with the difference that CuO (1 wt.%) was added before the second attrition-milling. The calcination temperatures were set at 740 and 990°C , respectively, when Nb_2O_5 HJD and Alfa were used.

Specific area of the powders was determined using BET method (Flowsorb II 2300, micromeritics model). ANT phase formation was investigated on raw materials mixture using thermo differential analysis coupled with a thermo gravimetric analysis (DTA/TGA: SDT 2960, TA Instruments Model) on raw material mixture. Phase identification of the samples was performed using X-ray diffractometry (XRD; XCPs 120 INEL) at room temperature.

Microstructures were examined using scanning electron microscope for observation (SEM S4000, Hitachi model) and energy-dispersive X-ray spectroscopy for mapping (ABT/TOPCON 150F model using Noran EDS system) and Auger electron spectroscopy for observation and mapping (AES with the nanoprobe Auger PHI 680). This analysis was carried out on grinded and polished pellets. To determine the grain size,

samples were thermally etched for 10 min at the sintering temperature and then rapidly cooled to room temperature.

Sintering was investigated by measuring the density of the sintered samples using the Archimede's method and Thermo Mechanical Analysis (Setaram TMA 92).

Dielectric constant and losses were measured from 40 Hz to 10 kHz range with an impedance analyzer (4294A, Agilent model). Dielectric properties in the microwave range were determined by the dielectric resonator method⁴ on a network analyser (HP 85-10, Agilent model) in the transmission mode. Temperature dependence of dielectric constant was obtained at 100 kHz between -25 and $+150^\circ\text{C}$ by measuring the capacitance of a metalized disk.

Table 2

Specific area at different stage of the preparation

Powders	S (m^2/g)
After first milling	
Mixture with Nb_2O_5 Alfa	1.7 ± 0.1
Mixture with Nb_2O_5 HJD	3.5 ± 0.1
After second milling	
ANT with Nb_2O_5 Alfa	1.3 ± 0.1
ANT with Nb_2O_5 HJD	3.1 ± 0.1

3. Results and discussion

3.1. Physico-chemical characterizations

First, specific area was measured at different stage of the preparation: on raw materials, after the first milling and after the second milling (Table 2).

ANT phase formation using Nb₂O₅ HJD was investigated by DTA/TGA on raw materials mixture up to 900 °C in air. XRD analysis performed on calcinated samples is also reported in Fig. 1.

A first mixture: (1/2)Ag₂O–(1/4)Nb₂O₅–(1/4)Ta₂O₅ composition was studied (Fig. 1a and c). The mass loss observed at 200 and 400 °C is related, respectively, to H₂O loss and Ag₂O decomposition. Once metallic silver is appeared, the ANT phase formation begins at about 430 °C and finishes around 820 °C.

After calcining at 620 °C, XRD analysis revealed the presence of raw materials with ANT phase. At 700 °C, ANT phase is predominant with a few impurities whereas at 740 °C, ANT phase was completely formed.

In order to investigate the role of CuO on the phase formation, a second mixture was considered: 0.5Ag₂O–0.25Ta₂O₅–0.232Nb₂O₅–0.037CuO (Fig. 1b and d). Similar phenomena are observed, except that the phase formation starts at lower temperature (420 °C). XRD analyses confirm this result. At 500 °C, the ANT phase is already present and it is completely formed at 610 °C.

The effect of CuO is very impressive at such low temperature.

Sintering conditions were optimized according to temperature and atmosphere. Full densification and small grain size were obtained at 880 °C in air and 915 °C in oxygen. O₂ sintered samples present the highest density although the densification starts

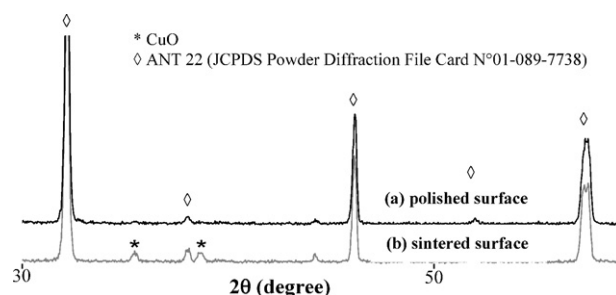


Fig. 2. XRD patterns of the polished surface (a) and the as-sintered surface (b) for Ag₂O deficiency samples.

30 °C lower. TMA analyses in air and in O₂ have confirmed this difference of kinetics.

3.2. Structure and microstructure

XRD analysis was performed on sintered samples (Fig. 2). Significant differences were found between the surface and the inside of the sample. The inside was only single-phased ANT whereas CuO was detected on the surface. EDS and AES elemental mapping realised on samples polished and thermally etched pellets have confirmed CuO exodiffusion.

3.3. Relations between electromagnetic properties and microstructure

Electromagnetic measurements were performed between 1 and 3 GHz using the Hakki–Coleman method for copper substitutions and copper oxide additions (Table 3). The best microwave dielectric properties were obtained for Ag₂O deficiency samples. With a permittivity of 415 and a $Q \times f = 610$ GHz, CuO for

Table 3
dielectric properties at 1.6 GHz using Nb₂O₅ HJD (fine grain) and Nb₂O₅ Alfa (large grain)

Compositions	CuO substitutions						CuO-additions	
	Ta ₂ O ₅ (0.5Ag ₂ O–0.25Nb ₂ O ₅ –0.232Ta ₂ O ₅ –0.037CuO)		Nb ₂ O ₅ (0.5Ag ₂ O–0.25Ta ₂ O ₅ –0.232Nb ₂ O ₅ –0.037CuO)		Ag ₂ O (0.482Ag ₂ O–0.037CuO–0.25Ta ₂ O ₅ –0.25Nb ₂ O ₅)		0.5Ag ₂ O–0.25Nb ₂ O ₅ –0.25Ta ₂ O ₅ –0.037CuO	
	$T_s = 880^\circ\text{C}$ (atm: air)	$T_s = 915^\circ\text{C}$ (atm: O ₂)	$T_s = 880^\circ\text{C}$ (atm: air)	$T_s = 915^\circ\text{C}$ (atm: O ₂)	$T_s = 880^\circ\text{C}$ (atm: air)	$T_s = 915^\circ\text{C}$ (atm: O ₂)	$T_s = 880^\circ\text{C}$ (atm: air)	$T_s = 915^\circ\text{C}$ (atm: O ₂)
Nb ₂ O ₅ HJD								
d (g cm ^{–3})	7.45	7.65	7.35	7.8	7.55	7.7	7.35	7.75
K (1.6 GHz)	455	465	440	465	395	415	390	415
$Q \times f$ (GHz)	260	285	260	355	530	610	405	465
Compositions	CuO substitutions						CuO-additions	
	Ta ₂ O ₅ (0.5Ag ₂ O–0.25Nb ₂ O ₅ –0.232Ta ₂ O ₅ –0.037CuO)		Nb ₂ O ₅ (0.5Ag ₂ O–0.25Ta ₂ O ₅ –0.232Nb ₂ O ₅ –0.037CuO)		Ag ₂ O (0.482Ag ₂ O–0.037CuO–0.25Ta ₂ O ₅ –0.25Nb ₂ O ₅)		0.5Ag ₂ O–0.25Nb ₂ O ₅ –0.25Ta ₂ O ₅ –0.037CuO	
	$T_s = 900^\circ\text{C}$ (atm: air)	$T_s = 930^\circ\text{C}$ (atm: O ₂)	$T_s = 900^\circ\text{C}$ (atm: air)	$T_s = 930^\circ\text{C}$ (atm: O ₂)	$T_s = 900^\circ\text{C}$ (atm: air)	$T_s = 930^\circ\text{C}$ (atm: O ₂)	$T_s = 900^\circ\text{C}$ (atm: air)	$T_s = 930^\circ\text{C}$ (atm: O ₂)
Nb ₂ O ₅ Alfa								
d (g cm ^{–3})	7.55	7.65	7.6	7.8	7.5	7.65	7.7	7.8
K (1.6 GHz)	440	520	440	550	385	415	415	435
$Q \times f$ (GHz)	240	490	290	310	355	525	310	465

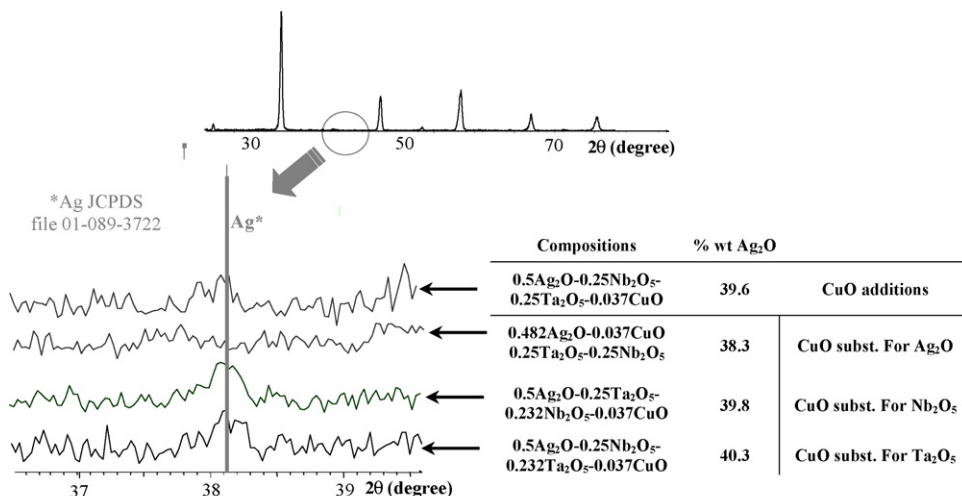


Fig. 3. Evidence of silver presence using XRD.

Ag₂O substituted samples sintered in O₂ have better dielectric properties than CuO added samples.

To understand these results, XRD and EDS analysis were performed. Except for Ag substitutions, all samples contain a metallic silver secondary-phase (JCPDS powder diffraction file card no. 01-089-3722) after calcination and sintering (Fig. 3). Elemental mapping led on Nb₂O₅ and Ta₂O₅ deficiency samples have clearly confirmed the presence of large metallic Ag particles (30 μm). For Ag₂O deficiency samples, only weak traces of metallic Ag were detected. So, higher dielectric losses could be attributed to the presence of metallic Ag.

Concerning the microstructure, samples where Nb₂O₅ or Ta₂O₅ was replaced by CuO have smaller grain size. This could be explained by the presence of metallic silver that limits grain growth.

Moreover, EDS chemical analysis performed on copper substituted samples have revealed that the distribution of copper inside the grain is homogeneous (Fig. 4). Copper mapping has

not shown any copper concentration at grain boundary which confirms that copper enters inside the solid solution. Auger nanoprobe analysis has confirmed this result.

To ensure the electroneutrality, Cu²⁺ ions must be located both on the A and B sites according to the relation:

$$(3/4)\text{Ag}^+ [\text{A site}] + 1/4 (\text{Nb}^{5+} \text{ or } \text{Ta}^{5+}) [\text{B site}] \rightleftharpoons (3/4)\text{Cu}^{2+} [\text{A site}] + (1/4)\text{Cu}^{2+} [\text{B site}]$$

This could explained why more metallic silver is observed in Nb₂O₅ and Ta₂O₅ deficiency samples than in Ag₂O deficiency samples.

Low frequency dielectric properties were evaluated from 40 Hz to 10 kHz (Fig. 5). In accordance with microwave measurement, low losses were obtained for O₂ sintered samples and for Ag₂O deficiency samples. No difference was noticed between copper substituted and CuO added samples.

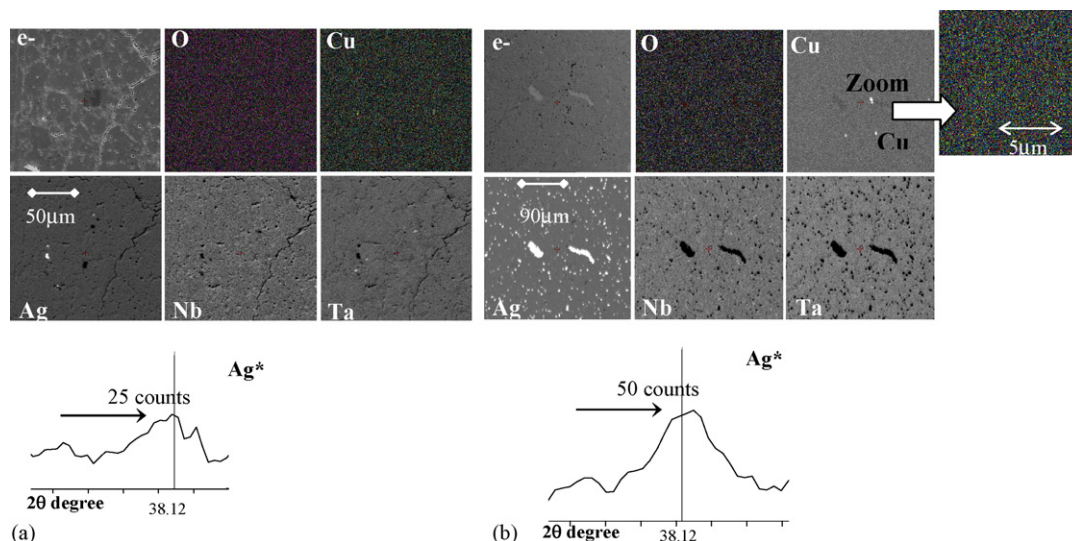
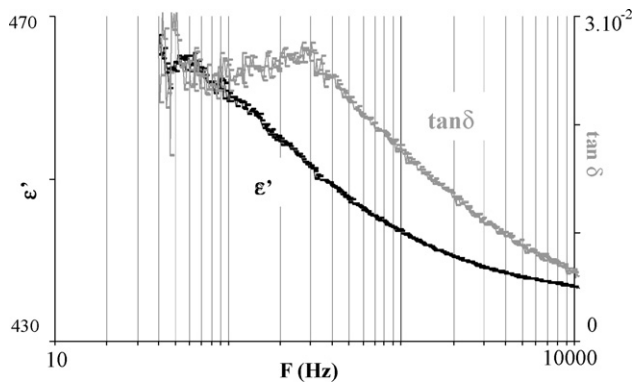


Fig. 4. EDS (elemental mapping: e⁻, O, Cu, Ag, Nb, Ta and XRD) on sintered samples; (a) 0.482Ag₂O-0.25Nb₂O₅-0.25Ta₂O₅-0.037CuO; (b) 0.5Ag₂O-0.232Nb₂O₅-0.25Ta₂O₅-0.037CuO.

Table 4

TCC and K_{\max} values measured at 100 kHz between -25 and 150 °C (samples made from Nb_2O_5 HJD)

Compositions	$T_s = 880\text{ }^{\circ}\text{C}$ air				$T_s = 900\text{ }^{\circ}\text{C}$ O_2			
	TCC ₁ (ppm/ $^{\circ}\text{C}$)	TCC ₂ (ppm/ $^{\circ}\text{C}$)	K_{max} at T ($^{\circ}\text{C}$)		TCC ₁ (ppm/ $^{\circ}\text{C}$)	TCC ₂ (ppm/ $^{\circ}\text{C}$)	K_{max} at T ($^{\circ}\text{C}$)	
CuO substitutions								
Ta ₂ O ₅ (0.5Ag ₂ O–0.25Nb ₂ O ₅ –0.232Ta ₂ O ₅ –0.037CuO)	415	−710	550	22	835	795	480	32
Nb ₂ O ₅ (0.5Ag ₂ O–0.25Ta ₂ O ₅ –0.232Nb ₂ O ₅ –0.037CuO)	165	−390	445	−17	255	−875	335	9
Ag ₂ O (0.482Ag ₂ O–0.037CuO–0.25Ta ₂ O ₅ –0.25Nb ₂ O ₅)	1215	−1235	515	54	440	−955	405	9
CuO additions								
0.5Ag ₂ O–0.25Nb ₂ O ₅ –0.25Ta ₂ O ₅ –0.037CuO	370	−845	335	36	810	−1430	405	48

Fig. 5. Permittivity and dielectric loss tangent from 40 Hz to 10 kHz for Ag_2O deficiency samples sintered at 880 °C in air.

“ K and $\tan \delta$ as a function of frequency” curves were very similar and decreased very slightly with frequency.

Table 4 gives the temperature coefficient of capacitance (TCC) between -25 and $+150$ °C for all the samples. K increases from -25 °C to T corresponding to K_{\max} and go down from T to $+150$ °C. So, the temperature coefficient is defined by the following relation:

$$\text{TCC} = \frac{\Delta K}{K_{\text{RT}} \Delta T}$$

where $\Delta K = K(T_{\max} \text{ or } T_{\min}) - K_{\max}$ and $\Delta T = (T_{\max} \text{ or } T_{\min}) - T(K_{\max})$.

The highest TCC was obtained for Ag_2O deficiency samples whereas when Nb_2O_5 was replaced by CuO , TCC were the lowest.

4. Conclusions

Dielectric properties of CuO substituted and added ANT were compared. For Nb_2O_5 and Ta_2O_5 deficiency samples, EDS and XRD analysis indicated the presence of metallic silver. This can probably be explained by the location of a part of Cu in the A site of the crystal. EDS and AES analyses confirmed that copper was located inside the grain. The metallic silver present in these samples was prejudicial for electromagnetic losses.

With a permittivity of 415 and a $Q \times f = 610$ GHz, Ag_2O deficiency samples present better dielectric properties than CuO added samples. These characteristics are very promising for the radio-frequency/microwave applications.

References

1. Valant, M., Suvorov, D. and Meden, A., $\text{AgNb}_{1-x}\text{Ta}_x\text{O}_3$ -new high permittivity microwave ceramics. Part I. Crystal structures and phase decomposition relations. *J. Am. Ceram. Soc.*, 1999, **82**, 81–87.
2. Valant, M., Suvorov, D., Hoffmann, C. and Sommariva, H., $\text{Ag}(\text{Nb,Ta})\text{O}_3$ -based ceramics with suppressed temperature dependence of permittivity. *J. Eur. Ceram. Soc.*, 2001, **21**, 2647–2651.
3. Kim, H. T., Shrout, T., Randall, C. and Lanagan, M., Low-temperature sintering and dielectric properties of $\text{Ag}(\text{Nb,Ta})\text{O}_3$ composite ceramics. *J. Am. Ceram. Soc.*, 2002, **85**, 2738–2744.
4. Hakki, B. W. and Coleman, P. D., A dielectric resonator method of measuring inductive capacities in the millimeter range. *IRE Trans. Microwave Theory Tech.*, 1960, 402.